Observation of Two-Dimensional Surface Solitons

Article *in* Physical Review Letters · April 2007

DOI: 10.1103/PhysRevLett.98.123903 · Source: PubMed

6 authors, including:

Xiaosheng Wang
Xiangya Hospital of Central South University
32 PUBLICATIONS **872** CITATIONS
SEE PROFILE

Anna Bezryadina
California State University, Northridge
60 PUBLICATIONS **947** CITATIONS
SEE PROFILE

Zhigang Chen
San Francisco State University
496 PUBLICATIONS **10,865** CITATIONS
SEE PROFILE

Konstantinos G Makris
University of Crete
127 PUBLICATIONS **9,899** CITATIONS
SEE PROFILE

Observation of Two-Dimensional Surface Solitons

Xiaosheng Wang,[1] Anna Bezryadina,[1] and Zhigang Chen[1,2]
[1]*Department of Physics and Astronomy, San Francisco State University, California 94132 USA*
[2]*TEDA Applied Physics School, Nankai University, Tianjin 300457 China*

K. G. Makris, D. N. Christodoulides, and G. I. Stegeman
College of Optics and Photonics, CREOL & FPCE, Univ. of Central Florida, Orlando, Florida 32816 USA
(Received 11 December 2006; published 21 March 2007)

We report the first experimental observation of two-dimensional surface solitons at the boundaries (edges or corners) of a finite optically induced photonic lattice. Both in-phase and gap nonlinear surface self-trapped states were observed under single-site excitation conditions. Our experimental results are in good agreement with theoretical predictions.

DOI: 10.1103/PhysRevLett.98.123903 PACS numbers: 42.65.Tg, 42.65.Sf

Surface waves are ubiquitous wave phenomena that have been studied in diverse areas of physics such as acoustics, plasma, ocean physics, and geomechanics, to name just a few [1]. Electronic localized surface states were first predicted by Tamm and subsequently studied by Shockley in the 1930's [2], and have been demonstrated in a series of experiments ranging from semiconductor crystal surfaces to nanoengineered superlattices [3]. In optics, linear Tamm-Shockley-like surface waves were proposed in 1966 [4], but they were not observed until a decade later in experiments with AlGaAs multilayer structures [5].

Recently, optical self-trapped discrete surface waves (surface solitons) have aroused great interest [6–14]. This class of surface waves can be loosely interpreted as nonlinear defect modes with propagation eigenvalues located within the forbidden optical band gaps of a periodic structure [15]. Thus far, one-dimensional (1D) in-phase surface solitons, first predicted to exist at the edge of nonlinear self-focusing waveguide lattices [6], have been demonstrated experimentally in AlGaAs arrays [7]. Moreover, 1D surface gap or staggered solitons at the interface between a uniform medium and a self-defocusing waveguide array have also been analyzed [6,8] and demonstrated in both quadratic [9] and photorefractive nonlinear material systems [10,11]. Unlike their in-phase counterparts, these latter entities exhibit propagation eigenvalues located in the first photonic band gap (between the first and second Bloch bands) at the edge of the Brillouin zone. These studies extend the correspondence between optical surface waves and localized surface Tamm states into the nonlinear regime, since surface gap solitons can be viewed as the optical nonlinear analogues of Tamm states. Quite recently, theoretical studies of such surface solitons have been carried out in the two-dimensional (2D) domain where many interesting aspects associated with nonlinear surface waves are expected to be observed [12–14]. Despite these efforts, direct experimental observation of 2D surface solitons has remained a challenge due to experimental difficulties in fabricating 2D nonlinear lattices with a sharp edge. In fact, to our knowledge, 2D surface solitons have never been observed in any system.

In this Letter, we present the first experimental demonstration of 2D in-phase and gap surface solitons (2D nonlinear Tamm states) propagating along the boundaries of an optically induced 2D photonic lattice. The properties and characteristics of this class of waves are systematically investigated both experimentally and theoretically. The difference between the two types of surface solitons is clearly illustrated in our experiments by phase measurement as well as by monitoring their Fourier spectrum. In addition, surface solitons at the corner of a 2D lattice were also observed and compared to those existing away from the boundaries. These experimental results are corroborated by our theoretical analysis.

To create a 2D waveguide lattice, we use the optical induction method as used in discrete soliton experiments carried out in an infinite uniform lattice [16–18]. In our experimental setup [18–20], the lattice pattern is generated by periodic spatial modulation of a partial incoherent optical beam with an amplitude mask, which enables the generation of a square lattice pattern with a sharp edge or corner at the crystal input after proper imaging [Fig. 1(a)]. While the Talbot effect of the periodic intensity pattern is suppressed by using a diffraction element, the lattice edge or corner diffracts significantly in the linear region [Fig. 1(b)], as for the case of defect propagation in a 2D lattice [20]. With an appropriate level of nonlinearity (as controlled by lattice beam intensity, coherence, and polarization together with the bias field), the lattice edge or corner recovers and remains nearly invariant through a 10-mm long Ce:SBN photorefractive crystal [Fig. 1(c)]. Thus, an interface, although somewhat deformed, between the 2D waveguide lattice (of about 23 μm lattice spacing) and the continuous material is established in the biased crystal. To observe the linear and nonlinear propagation dynamics at the surface of the waveguide lattice, we launch an extraordinarily-polarized Gaussian probe beam (488 nm wavelength and 14 μm intensity FWHM) at the interface

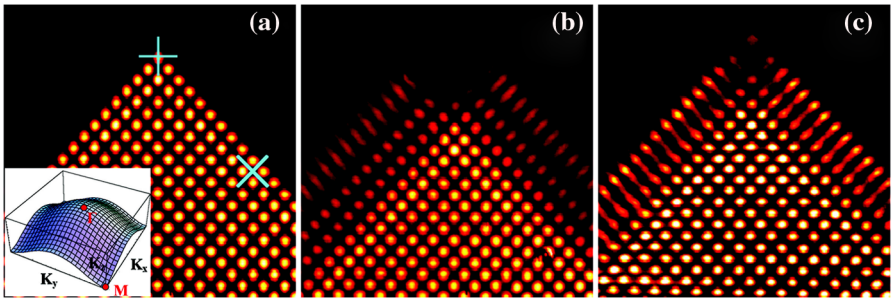

FIG. 1 (color online). Intensity patterns of a 2D square lattice at the input of the crystal (a) and the output of the crystal under linear (b) and nonlinear (c) propagation. The plus symbol in (a) marks the location for on-site excitation of corner solitons and the cross for off-site excitation of surface gap solitons. The insert in (a) illustrates the 1st band structure and high symmetry points.

into the crystal, without any tilting angle with respect to the lattice beam.

First, we apply a positive voltage to turn the crystal into a self-focusing medium, and demonstrate in-phase surface solitons propagating in the semi-infinite gap of the lattice. For comparison, the probe beam is sent to excite a single waveguide channel (on-site excitation) at or close to the edge [Figs. 2(a) and 2(d)] as well as far away from the boundary [Fig. 2(g)]. At a low bias field, the probe beam exciting the waveguide at the edge (i.e., the first row of the square lattice) experiences linear discrete diffraction [Fig. 2(b)]. The discrete diffraction in this case is stronger in the direction perpendicular to the lattice interface than in the direction parallel to it, which might arise from the surface enhanced reflection [7–11]. Similar diffraction behavior is observed when the probe beam excites a waveguide close to the lattice edge [Fig. 2(e)]. However, it is remarkably different when the probe beam excites a waveguide inside and far away from the lattice boundary, for which the symmetric discrete diffraction pattern [18] is observed [Fig. 2(h)]. At a high bias field, the probe beam undergoes nonlinear propagation. Under proper bias conditions (with an applied electric field of 2.2 kV/cm), self-action of the probe beam leads to localization of its intensity mostly in the waveguide it excites, forming a discrete soliton [15] [Figs. 2(c), 2(f), and 2(i)]. Again, the intensity pattern of the discrete soliton at surface [Fig. 2(c)] is asymmetric as compared to that inside the lattice [Fig. 2(i)]. We emphasize that the surface soliton is formed by the nonlinear self-action of the probe beam at the lattice edge. This is verified by comparing the instantaneous (before self-action) and steady-state (after self-action) intensity patterns of the probe beam, taking advantage of the noninstantaneous response of the photorefractive crystal. In fact, if we reduce the intensity of the probe beam significantly, it cannot form a soliton but rather experiences strong discrete diffraction at the surface. This is illustrated in Figs. 2(j) and 2(k) by 3D intensity plots, where a surface discrete soliton, as in Fig. 2(c), is formed in steady-state [Fig. 2(j)], but it cannot survive [Fig. 2(k)] when its intensity is reduced by a factor of about 8 under the same bias conditions.

We note that the propagation eigenvalues of the surface discrete solitons in Fig. 2 exist in the semi-infinite gap of the lattice, and thus the intensity peaks are located in the waveguide sites, and the main peak is in-phase with the adjacent ones. To verify this phase relation, a surface soliton [shown in Fig. 3(a)] is interfered with a tilted reference plane wave. The interference pattern is presented in Fig. 3(b), which shows an in-phase relation for the intensity spots in the direction parallel to the edge since the interference fringes through the main peak and the

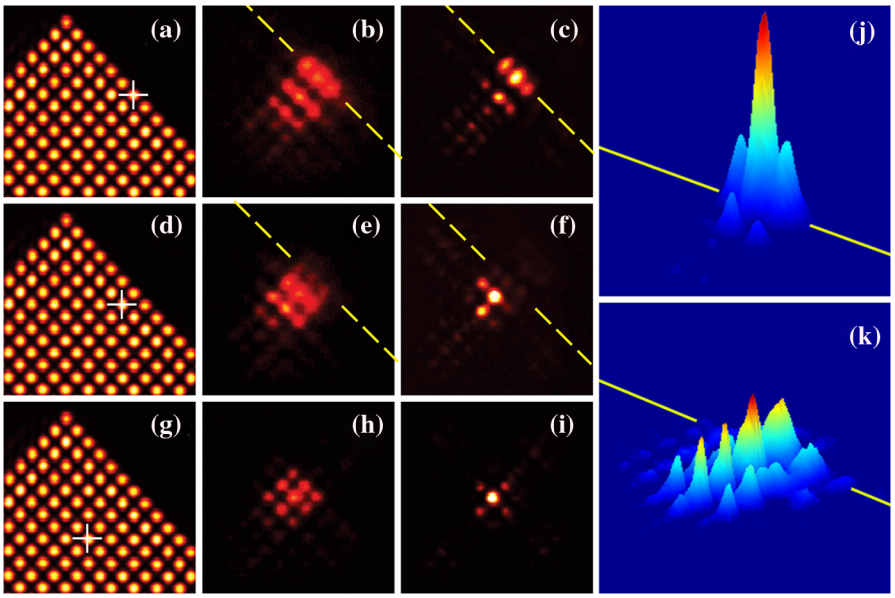

FIG. 2 (color online). Observation of discrete solitons at different locations relative to the lattice edge. The first column shows the lattice patterns with the waveguide excited by the probe beam marked by a plus. The second column shows linear discrete diffraction of the probe beam at a low bias field of 0.6 kV/cm. The third column shows soliton formation at a high bias field of 2.2 kV/cm. The fourth column shows the 3D intensity plots of a surface soliton (j) and the corresponding pattern when its intensity is reduced significantly under the same bias condition (k). (The added lines mark the interface between the lattice and continuous region of the crystal).

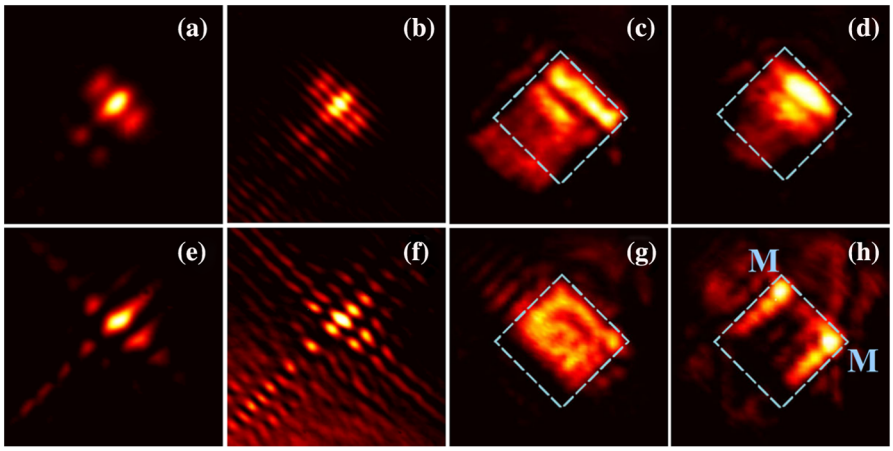

FIG. 3 (color online). Experimental results of in-phase (top) surface solitons and out-of-phase (bottom) surface gap solitons. First column shows the soliton intensity pattern; second column is the interference pattern between the soliton beam and a tilted plane wave; third and forth columns show the spatial spectra when the probe beam undergoes linear diffraction and nonlinear self-trapping, respectively. (The added squares mark the edge of the first Brillouin Zone).

adjacent intensity peaks are connected without shifting. This same in-phase relation is also verified for the direction perpendicular to the lattice edge due to different behavior of beam transport towards the waveguide lattice and the continuous region. When the surface soliton is formed, the spectrum reshapes, and the bright spot close to the center becomes more pronounced, indicating that the soliton originates from the Γ point in the 1st spectral band of the 2D lattice [21,22].

Next, we apply a negative voltage to turn the crystal into a self-defocusing medium and demonstrate 2D out-of-phase (staggered) surface solitons propagating in the first band gap of the ''backbone'' lattice [17,21]. Under a proper defocusing nonlinearity (with an applied electric field of -1.5 kV/cm), a surface gap soliton is observed with a single-beam excitation [off site excitation position is marked with a cross in Fig. 1(a), corresponding to an index maximum]. Such a surface gap soliton has its intensity mainly localized in the excitation position, but with long tails along the directions both perpendicular to and parallel with the lattice edge [Fig. 3(e)]. The ''staggered'' structure of the gap soliton is monitored again by the interference measurement of the phase [Fig. 3(f)] as well as the spectrum measurement in Fourier space [Figs. 3(g) and 3(h)]. The breaking and interleaving of interference fringes in Fig. 3(f) indicates a staggered phase relation of the surface gap soliton [10]. The spectrum for this soliton [Fig. 3(h)] is also dramatically different from that of in-phase surface solitons in the semi-infinite gap [Fig. 3(d)]. Since the gap soliton (with propagation constant located between the 1st and 2nd Bloch bands) is expected to originate from the four M-symmetry points of the 1st band, its spectrum should show four bright spots matching the four M points of the 1st Brillouin Zone [21,22]. However, for the surface gap soliton studied here which has a smooth tail into the continuous region but a modulated tail into the lattice region, the contribution to surface gap soliton from the lattice region shows clearly two bright spots [the top and right spots in Fig. 3(h)] matching the two M points of the 1st Brillouin Zone, while the contribution from the continuous region results in deformation of two M points [the bottom and left corners in Fig. 3(h)], thus making the entire spectrum to be asymmetric. Considering the deformed lattice surface as established in our experiment [Fig. 1], such asymmetry in the k-space spectrum corresponding to the formation of surface solitons seems to be more pronounced in experimental results [Fig. 3] than in numerical simulations presented below where a prefect lattice surface is assumed [Fig. 4].

Even so, the above experimental observations are corroborated by our numerical simulations using a normalized 2D saturable nonlinear Schrödinger equation with a semi-

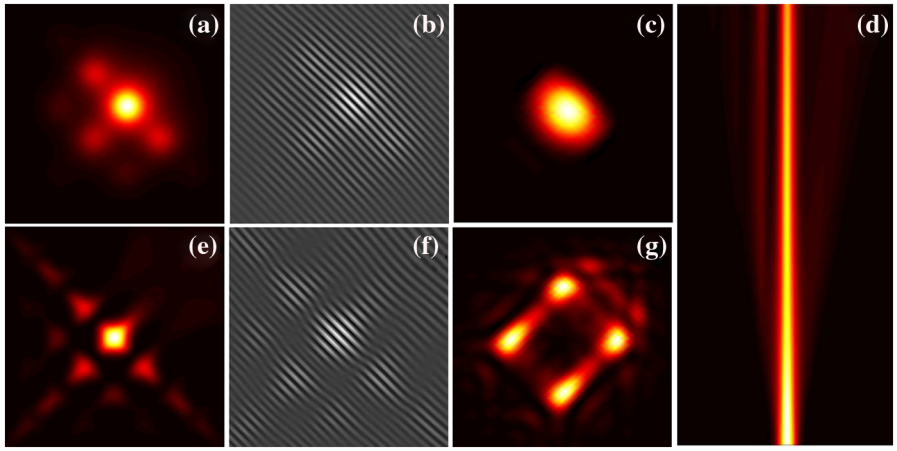

FIG. 4 (color online). Numerical results of in-phase (a)–(c) surface solitons and out-of-phase (e)–(g) surface gap solitons corresponding to Fig. 3. First column shows the soliton pattern; second column shows the interference pattern between the soliton beam and a tilted plane wave; third column shows the corresponding spatial spectra of the solitons. The right panel (d) shows 10-mm propagation of the surface gap soliton starting from bottom, with waveguide lattice located in the left side of the beam..

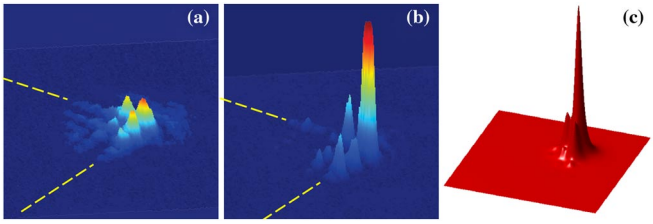

FIG. 5 (color online). Experimental (a), (b), and theoretical (c) results of in-phase discrete solitons formed at the corner of a 2D photonic lattice. (a) shows the discrete diffraction at low nonlinearity, (b) shows the formation of a corner soliton at high nonlinearity, and (c) shows corresponding solution for the corner soliton. Location for on-site excitation of corner solitons is indicated in Fig. 1(a).

infinite index potential [12]. Our analysis leads to solutions for surface in-phase solitons and surface gap solitons existing at the edge of the semi-infinite 2D square lattice. Typical simulation results obtained using parameters close to those from experiments are presented in Fig. 4, where the top panels are for in-phase surface solitons obtained with focusing nonlinearity and the bottom panels are for staggered gap solitons obtained with defocusing nonlinearity. Figures 4(a) and 4(e) show the patterns of the surface solitons corresponding to Figs. 3(a) and 3(e), and Figs. 4(b) and 4(f) show the interference patterns with a tilted plane wave corresponding to Figs. 3(b) and 3(f), and Figs. 4(c) and 4(g) show the theoretical Fourier spectra of the solitons corresponding to Figs. 3(d) and 3(h), respectively. On the right panel [Fig. 4(d)], propagation of the surface gap soliton up to 10 mm is illustrated. These numerical results are in good agreement with experimental observations.

The results presented above (both the phase structure and the distinctive Fourier spectrum) clearly indicate that a single Gaussian probe beam could evolve not only into a surface soliton in the semi-infinite gap but also to a surface gap soliton in the first band gap by single-channel excitation at or near the lattice edge. For a 2D lattice, the required lattice potential (or the induced index changes) for opening the first band gap is quite different between the focusing and defocusing lattices [21]. In our experiment, although the intensity ratio (i.e., the lattice-to-probe-beam peak intensity ratio) is similar (about 2) for both cases, the lattice potential we used to form surface gap solitons is much higher than that for the in-phase surface soliton. This is achieved by making the normalized lattice intensity about 7 times higher for the defocusing case as compared to the focusing case. Experimentally, the estimated index change for the defocusing lattice is about 1.5×10^{-4}. Under such a condition, the first gap should be open even in the backbone lattice [21], thus enabling our observation of surface gap solitons. When we decrease the lattice potential (either by decreasing the bias field or the normalized lattice intensity), we find that the probe beam simply cannot evolve into a surface gap soliton.

Finally, we present results of surface solitons observed at the corner of a 2D square lattice. To observe the formation of a corner soliton, a probe is sent for on-site excitation of the lattice site at the corner [marked by a plus symbol in Fig. 1(a)]. Although the corner is slightly deformed [Fig. 1(c)], discrete diffraction at low nonlinearity Fig. 5(a) and trapping at high nonlinearity Fig. 5(b) are observed. In the theoretical model, we have also found solutions for such corner solitons. Figure 5(c) shows the 3D plot of the corner soliton solution found using parameters corresponding to that of Fig. 5(b). We emphasize that such corner solitons have no analog in the 1D domain.

In summary, we have reported the first experimental observation of the 2D discrete surface solitons and surface gap solitons at the interface between an optically induced 2D waveguide lattice and a continuous medium.

This work was supported by NSF, AFOSR, PRF, and NSFC.

[1] S. V. Biryukov, *Surface Acoustic Wave in Inhomogenous Media* (Springer, New York, 1995); S. R. Massel, *Ocean Surface Waves: Their Physics and Prediction* (World Scientific, Singapore, 1996).
[2] I. E. Tamm, Z. Phys. **76**, 849 (1932); W. Shockley, Phys. Rev. **56**, 317 (1939).
[3] W. H. Brattain, Phys. Rev. **72**, 345 (1947); H. Ohno *et al.*, Phys. Rev. Lett. **64**, 2555 (1990); A. B. Henriques *et al.*, Phys. Rev. B **61**, R13369 (2000).
[4] D. Kossel, J. Opt. Soc. Am. **56**, 1434 (1966).
[5] P. Yeh *et al.*, Appl. Phys. Lett. **32**, 104 (1978).
[6] K. G. Makris *et al.*, Opt. Lett. **30**, 2466 (2005).
[7] S. Suntsov *et al.*, Phys. Rev. Lett. **96**, 063901 (2006).
[8] Y. V. Kartashov *et al.*, Phys. Rev. Lett. **96**, 073901 (2006).
[9] A. Siviloglou *et al.*, Opt. Express **14**, 5508 (2006).
[10] C. R. Rosberg *et al.*, Phys. Rev. Lett. **97**, 083901 (2006).
[11] E. Smirnov *et al.*, Opt. Lett. **31**, 2338 (2006).
[12] K. G. Makris *et al.*, Opt. Lett. **31**, 2774 (2006).
[13] Y. V. Kartashov *et al.*, Opt. Express **14**, 4049 (2006); Opt. Lett. **31**, 2172 (2006).
[14] R. A. Vicencio *et al.*, http://arxiv.org/abs/nlin/0610049.
[15] D. N. Christodoulides and R. I. Joseph, Opt. Lett. **13**, 794 (1988); H. S. Eisenberg *et al.*, Phys. Rev. Lett. **81**, 3383 (1998); D. N. Christodoulides *et al.*, Nature (London) **424**, 817 (2003).
[16] N. K. Efremidis *et al.*, Phys. Rev. E **66**, 046602 (2002).
[17] J. W. Fleischer *et al.*, Nature (London) **422**, 147 (2003); D. Neshev *et al.*, Opt. Lett. **28**, 710 (2003).
[18] H. Martin *et al.*, Phys. Rev. Lett. **92**, 123902 (2004).
[19] Z. Chen and K. McCarthy, Opt. Lett. **27**, 2019 (2002).
[20] I. Makasyuk *et al.*, Phys. Rev. Lett. **96**, 223903 (2006).
[21] N. K. Efremidis *et al.*, Phys. Rev. Lett. **91**, 213906 (2003).
[22] D. Trager *et al.*, Opt. Express **14**, 1913 (2006).